

[advances.sciencemag.org/cgi/content/full/6/48/eabb8675/DC1](https://advances.sciencemag.org/cgi/content/full/6/48/eabb8675/DC1)

## Supplementary Materials for

### **Direct observation of nanoparticle-surfactant assembly and jamming at the water-oil interface**

Yu Chai, Jaffar Hasnain, Kushaan Bahl, Matthew Wong, Dong Li, Phillip Geissler, Paul Y. Kim, Yufeng Jiang, Peiyang Gu, Siqi Li, Dangyuan Lei, Brett A. Helms, Thomas P. Russell\*, Paul D. Ashby\*

\*Corresponding author. Email: [tprussell@lbl.gov](mailto:tprussell@lbl.gov) (T.P.R.); [pdashby@lbl.gov](mailto:pdashby@lbl.gov) (P.D.A.)

Published 25 November 2020, *Sci. Adv.* **6**, eabb8675 (2020)

DOI: [10.1126/sciadv.abb8675](https://doi.org/10.1126/sciadv.abb8675)

#### **The PDF file includes:**

In situ AFM imaging  
Figs. S1 to S6  
Table S1  
Legends for movies S1 to S3

#### **Other Supplementary Material for this manuscript includes the following:**

(available at [advances.sciencemag.org/cgi/content/full/6/48/eabb8675/DC1](https://advances.sciencemag.org/cgi/content/full/6/48/eabb8675/DC1))

Movies S1 to S3

## AFM imaging

Silicon wafers with <100> orientation (University Wafer Inc.) were diced into square pieces 0.5 cm × 0.5 cm. The silicon piece and a larger diameter polytetrafluoroethylene (PTFE) washer were glued to a magnetic puck using epoxy. The purpose of the PTFE disk was to confine the water phase to the silicon substrate without wetting the metal puck. The epoxy was allowed to cure overnight.

Prior to experiments, all substrates and the AFM tip holder were washed thoroughly with pure water (18.2 MΩ·cm, Milli-Q), acetone, and toluene followed by drying under nitrogen. Immediately before use, substrates, AFM tip holder, and AFM tips (Biolever mini or AC40, Olympus) were cleaned in a UV Ozone tool for 10 minutes. The hydrophilic surface created by UV Ozone cleaning was especially crucial for the AFM tip to avoid contamination when interacting with the oil-water interface from the aqueous side.

A small oil droplet ~1 mm in diameter and ~100 nL in volume was placed in the middle of the silicon substrate. Due to the high viscosity of the oil, a pipette tip was used to deliver the oil by dipped in the oil solution and repeatedly touching the tip to another silicon piece. Near the tenth touch, the droplet volumes are consistent and one droplet is placed on the substrate used for imaging. The sample was then placed in a vacuum chamber to degas and equilibrate for 10 minutes. Subsequently, the sample was placed on the Cypher ES scanner (Oxford Instruments) and 40 μL of aqueous solution added to completely cover the oil droplet. In the meantime, another 20 μL of aqueous solution was used to wet the AFM tip and tip holder. Then, the tip holder was manually lowered so that the NP solution from the tip holder touched the substrate, forming a water bridge. This led to a typical three-phase contact angle (water-oil-substrate) of 45°.

All in situ AFM imaging experiments used AC mode, where the AFM tip oscillation was driven by a piezo in the tip holder. While photothermal excitation leads to more consistent cantilever oscillation, the additional heating resulted in severe bubble formation in the oil phase even with extensive degassing. It is worth mentioning that even the IR laser used for the cantilever deflection detection could induce bubbles. For tip approach, the free amplitude and setpoint were set to ~4.5 nm and 3.3 nm respectively, where a typical sensitivity was 15 nm/V. Due to squeeze-film damping, the free amplitude decreased during tip approach and led to false engagements. Further slight reductions in setpoint and re-engagement were used until a force curve characteristic of interaction with the oil-water interface was observed. During imaging, the free amplitude of the tip was set to a value between 3 nm and 15 nm with a setpoint value close to the free amplitude (typically > 90% ) so that minimal forces were applied to the sample. It was found that a large free amplitude deformed the interface but using a small free amplitude led to oscillations in the amplitude signal if there was substantial adhesion between the AFM tip and the underlying oil phase. As a result, it was preferred to start with a small free amplitude as new tips are more hydrophilic and less likely to stick to the interface and induce oscillations. However, as the imaging quality degraded, the free amplitude was set to a higher value. Also, during imaging, the oil droplet rounded due to an increase in the three-phase contact angle (water-oil-substrate). As a result, the height increase of the water-oil interface could be even larger than the working range of the piezo (4 μm). In this case, a short increase of the setpoint to retract the sample followed by lifting the tip holder with the stepper motors was conducted to keep the surface within the range of the Z piezo.

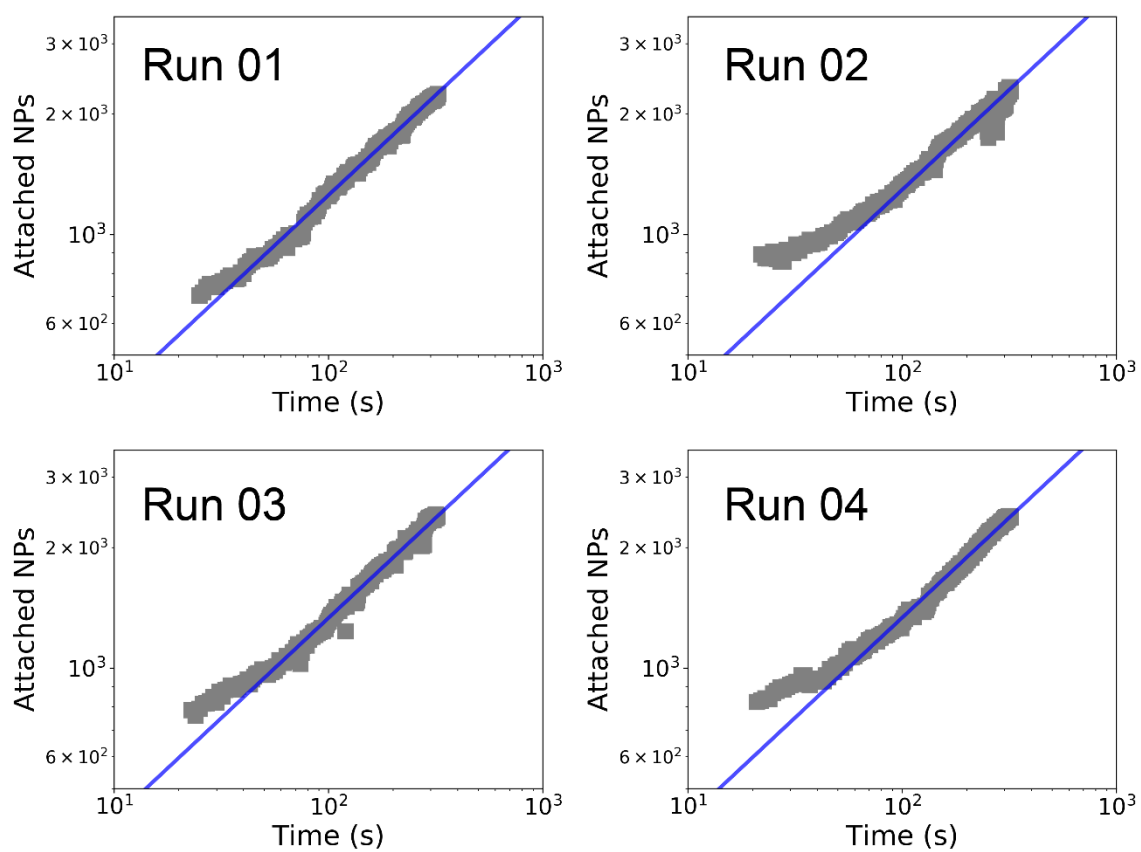


**Figure S1. Different runs of free attachment of 500 nm NPs to the water-oil interface.** The data are fit with a power law of 0.5 (blue solid lines) and show the same time dependence. The experimental condition is the same as that of Fig. 1C.

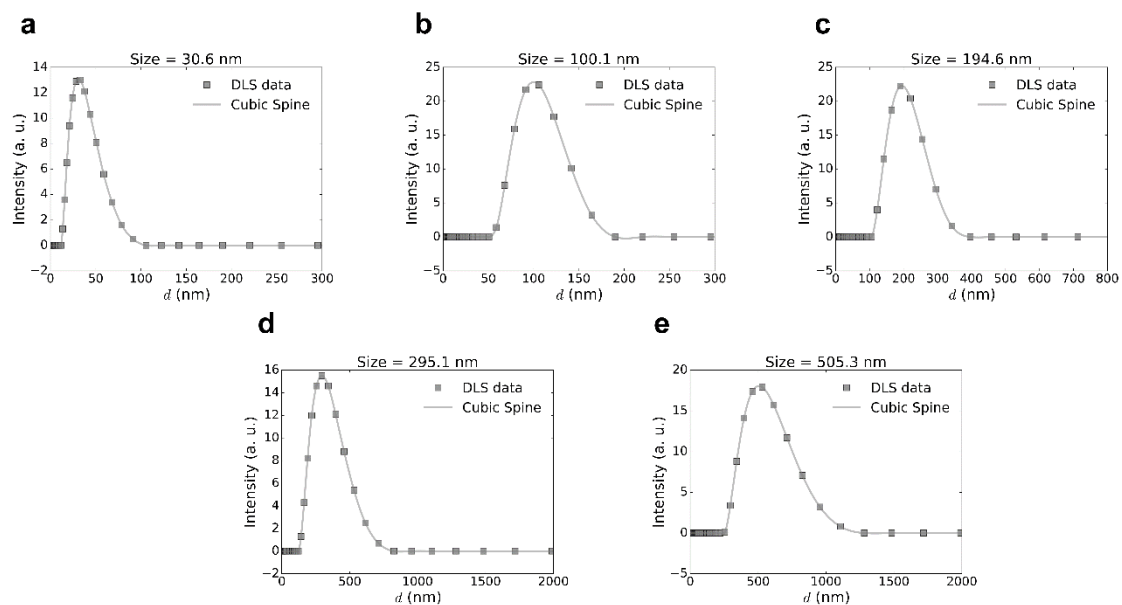


**Figure S2. Dynamic light scattering measurement of the different sized NPs used in this study. (A) 30 nm, (B) 100 nm, (C) 200 nm, (D) 300 nm, and (E) 500 nm, where the mean values are shown on top of each plot.**

### Binding Energy Calculations:

The energy of the NP at the oil-water interface can be separated into three components: the interaction with the oil phase,  $E_{PO}$ , the interaction with the aqueous phase,  $E_{PW}$ , and displacement of the oil-water interface by the particle,  $E_{OW}$ . Combining the three terms and solving for the energy minimum we find that at the equilibrium position the contact angle of the NP is related to the respective surface energies by the equation,  $\Delta\gamma = \gamma_{OW}\cos\theta$ , where  $\Delta\gamma$  is the difference between the NP-surfactant/oil surface energy,  $\gamma_{PO}$ , and the NP-aqueous phase surface energy,  $\gamma_{PW}$ . The oil-aqueous phase interfacial tension is  $\gamma_{OW}$ . The binding energy,  $E_B$ , of the NP to the interface is the energy difference between the energy minimum and the energy when the particle is completely transferred to one of the phases,  $E_B = \pi R^2\gamma_{OW}(1 - \cos\theta)^2$ . The values for the particles measured in Fig 1. of the main text are found in the following table using the interfacial tension value,  $23 \text{ mN} \cdot \text{m}^{-1}$ , for the surfactant oil solution and water in Fig. S3.

NP fit radius	NP fit position in oil phase	Contact Angle	$\Delta\gamma$	$E_B$
145 nm	113 nm	39°	18 $\text{mJ} \cdot \text{m}^{-2}$	$7.4 \times 10^{-17} \text{ J}$
55 nm	25 nm	63°	10 $\text{mJ} \cdot \text{m}^{-2}$	$6.5 \times 10^{-17} \text{ J}$
55 nm	28 nm	60°	12 $\text{mJ} \cdot \text{m}^{-2}$	$5.3 \times 10^{-17} \text{ J}$

**Table S1.** Table of fit results and binding energy calculations for NPs in Figure 1 of main text.

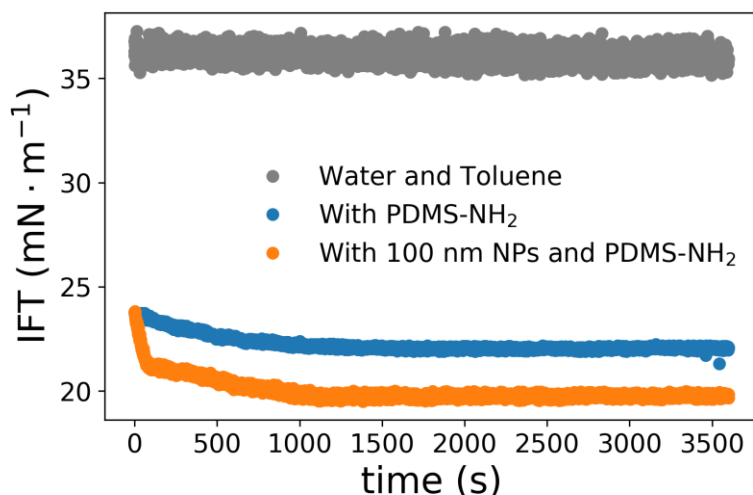


**Figure S3. Dynamic interfacial tension between water and toluene.** (Grey) Water-toluene, (Blue) Toluene phase with 10% w/w PDMS-NH<sub>2</sub>, (Orange) Water phase with 100 nm NPs (5 mM MES pH 6.5) and toluene phase with 10% w/w PDMS-NH<sub>2</sub>. The pure water and toluene interface has a constant interfacial tension value of  $\sim 36 \text{ mN} \cdot \text{m}^{-1}$ . In the presence of PDMS-NH<sub>2</sub> in toluene, it reduces to  $\sim 23 \text{ mN} \cdot \text{m}^{-1}$ . With both NPs and PDMS-NH<sub>2</sub>, interfacial tension further reduces to less than  $\sim 20 \text{ mN} \cdot \text{m}^{-1}$ .

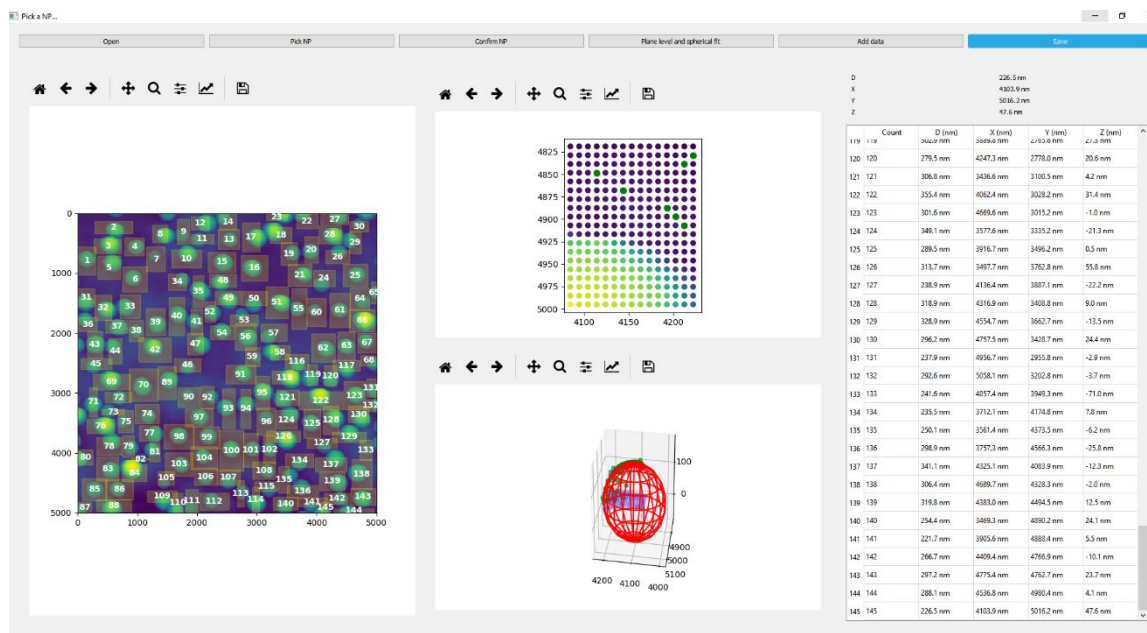


**Figure S4. Screenshot of the GUI of a single particle analysis script.** This script was used to extract the three-dimensional information of NPs assembled at the water-oil interface showing the pick and fitting of NPs, which can be further used for single particle analysis from any in situ AFM based experiments. This software is available upon request.

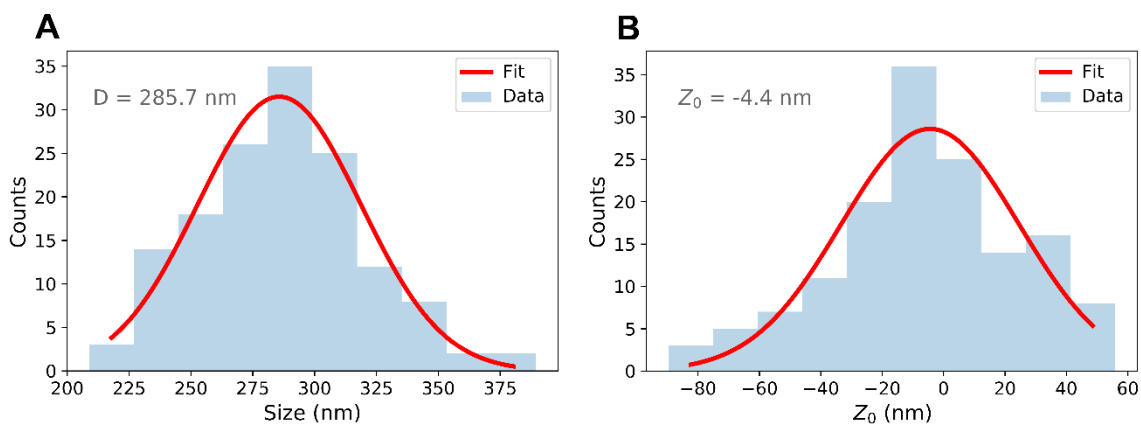


**Figure S5. Histograms of particles size and position relative to the apices of 30 nm NPs in the water-oil interface as measured by AFM. (A) Size and (B) center-of-mass distribution of 300 nm NPs in the sample in Fig. 3D at  $t_0$  obtained by our single particle analysis program shown in fig. S4, where the solid lines represent a fit using a normal distribution function.**

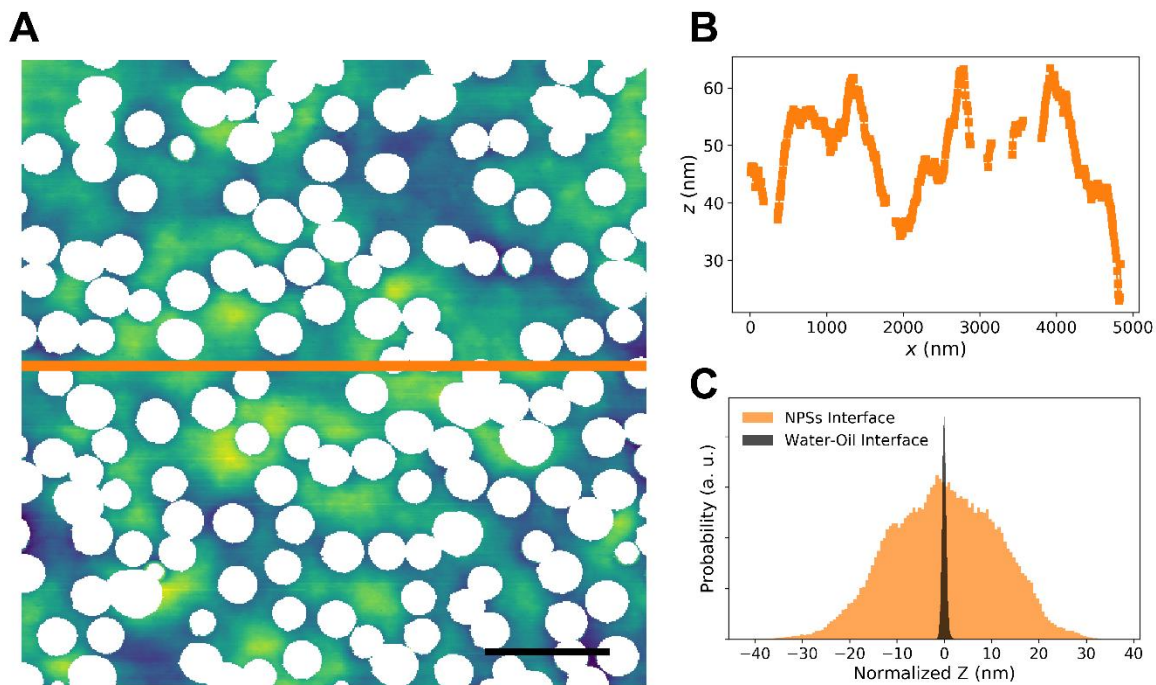


**Figure S6. AFM image showing roughness of NPS assemblies jammed at the water-oil interface.** (A) in situ AFM image of the water-oil interface of the sample in Fig. 3D at  $t_0$ . (B) The line profile shown in (A). (C) The height distribution of (A) compared to pure water-oil interface obtained by in situ AFM. Scale bar is 1  $\mu\text{m}$  and color scale is 80 nm.



## Movies

Movie S1 [Size: 35 MB] LCSM video shows the attachment of 500-nm (green) NPs to the interface covered with preassembled 70-nm (red) NPs, where the preassembly time is 30 minutes in this video.

Movie S2 [Size: 31 MB] LCSM video shows the attachment of 500-nm (green) NPs to the interface covered with preassembled 70-nm (red) NPs, where the preassembly time is 30 minutes in this video, and the sample has been washed with pure water.

Movie S3 [Size: 49 MB] LCSM video shows the coassembly of 70-nm (red) and-500 nm (green) NPs.